HHS Public Access

Author manuscript

Bone. Author manuscript; available in PMC 2016 December 01.

Published in final edited form as:

Bone. 2015 December ; 81: 152–160. doi:10.1016/j.bone.2015.07.012.

Bone's Responses to Mechanical Loading are Impaired in Type I Diabetes

Ashutosh Parajuli[#1], **Chao Liu**[#3], **Wen Li**[#2], **Xiaoyu Gu**[2], **Xiaohan Lai**[2], **Shaopeng Pei**[2], **Christopher Price**[1], **Lidan You**[3], **X. Lucas Lu**[1,2,*], and **Liyun Wang**[1,2,*]

[1]Department of Biomedical Engineering, University of Delaware, Newark, DE 19716, USA

[2]Department of Mechanical Engineering, University of Delaware, Newark, DE 19716, USA

[3]Department of Mechanical and Industrial Engineering, Institute of Biomaterials and Biomedical Engineering, University of Toronto, Ontario, Canada

[#] These authors contributed equally to this work.

Abstract

Diabetes adversely impacts many organ systems including the skeleton. Clinical trials have revealed a startling elevation in fracture risk in diabetic patients. Bone fractures can be life threatening: nearly 1 in 6 hip fracture patients die within one year. Because physical exercise is proven to improve bone properties and reduce fracture risk in non-diabetic subjects, we tested its efficacy in type 1 diabetes. We hypothesized that diabetic bone's response to anabolic mechanical loading would be attenuated, partially due to impaired mechanosensing of osteocytes under hyperglycemia. Heterozygous C57BL/6-Ins2^{Akita}/J (Akita) male and female diabetic mice and their age- and gender-matched wild-type (WT) C57BL/6J controls (7-month-old, N=5-7 mice/group) were subjected to unilateral axial ulnar loading with a peak strain of 3500 με at 2Hz and 3 min/day for 5 days. The Akita female mice, which exhibited a relatively normal body weight and a mild 40% elevation of blood glucose level, responded with increased bone formation (+6.5% in Ct.B.Ar, and 4 to 36-fold increase in Ec.BFR/BS and Ps.BFR/BS), and the loading effects, in terms of changes of static and dynamic indices, did not differ between Akita and WT females ($p \geq 0.1$). However, loading-induced anabolic effects were greatly diminished in Akita males, which exhibited reduced body weight, severe hyperglycemia (+230%), diminished bone formation (ΔCt.B.Ar: 0.003 vs. 0.030 mm^2, $p=0.005$), and suppressed periosteal bone appositions

[*]**Co-Corresponding authors:** Liyun Wang, Ph.D., Center for Biomedical Engineering Research, Department of Mechanical Engineering, 130 Academy Street, Newark, DE 19716, Tel: 302.831.2659, Fax: 302.831.3619, lywang@udel.edu, X. Lucas Lu, Ph.D., Center for Biomedical Engineering Research, Department of Mechanical Engineering, 130 Academy Street, Newark, DE 19716, Tel: 302.831.3581, Fax: 302.831.3619, xlu@udel.edu.
parajuli.ashutosh@gmail.com (AP); wenli@udel.edu (WL); laixhan@udel.edu (XL); davegu@udel.edu (XDG); shaopeng@udel.edu (SP), cprice@udel.edu (CP); youlidan@mie.utoronto.ca (LY)

Disclosures: All authors state that they have no conflicts of interest.

Author contributions: Study design—LW, XLL, LY; Data collection—AP, XL, XG, SP and CP for *in vivo* ulnar loading; and WL and XLL for *in vitro* studies; Data and statistical analysis—all authors; Data interpretation and manuscript drafting— LY, XLL and LW; LW takes responsibility for the integrity of the study.

(ΔPs.BFR/BS, p=0.02). Hyperglycemia (25mM glucose) was further found to impair the flow-induced intracellular calcium signaling in MLO-Y4 osteocytes, and significantly inhibited the flow-induced downstream responses including reduction in apoptosis and sRANKL secretion and PGE_2 release. These results, along with previous findings showing adverse effects of hyperglycemia on osteoblasts and mesenchymal stem cells, suggest that failure to maintain normal glucose levels may impair bone's responses to mechanical loading in diabetics.

Keywords

Akita diabetic mouse; ulnar mechanical loading; bone formation; osteocyte mechanosensitivity; fluid flow

Introduction

Obesity and diabetes are epidemic health problems associated with sedentary life-style and high-fat diets. According to the Center for Disease Control and Prevention's 2005-2008 National Health and Nutrition Examination Survey, 14% adults between age 45-64 and 27% adults older than 65 are diabetic. Diabetes causes serious health complications including heart disease, neuropathy, blindness, kidney failure, and lower-extremity amputations. It is the seventh leading cause of death in the United States (www.cdc.gov). However, the negative impacts of diabetes on bone health have not been well recognized until recently. In 2007, two meta-analyses of 13-16 large clinical trials showed a startling elevation in bone fracture risk for diabetic patients compared with normal population, which was 7-fold increase in type 1 diabetes (T1D, formerly called juvenile-onset diabetes) and 1.4-fold increase in type 2 diabetes (T2D, formerly called adult-onset diabetes) [1, 2]. Since nearly 1 in 6 patients with hip fracture died within one year [3], bone fractures can be life threatening. The risk is especially high for diabetic patients, whose impaired vasculature and wound healing capability contribute to increased mortality [4].

The mechanisms underlying the observed elevation in fracture risk among diabetics are not fully understood, although human and animal studies have documented bone defects such as retarded bone accrual and reduced bone size [5-7] (for T1D) and/or altered bone matrix [8, 9] and increased cortical porosities [10-12] (for T2D) [11, 12]. The fragile bone phenotypes have been recapitulated in various diabetic animal models [13-16]. On the cellular and molecular level, hyperglycemia and hormonal disturbances, present in both T1D and T2D [17, 18], were found to i) inhibit the proliferation and differentiation of bone marrow mesenchymal stem cells into bone-forming osteoblasts [19], ii) suppress osteoblast's functions [20, 21], and iii) increase nonenzymatic glycation of collagen (the major organic constitute of bone matrix) [8, 9, 15]. Paradoxically, long-term use of some diabetes treatments such as thiazolidinediones, a class of insulin-sensitizing drug including rosiglitazone and pioglitazone, was recently found to stimulate adipogenesis and inhibit osteogenesis, leading to even more bone deterioration [11, 22]. Thus, there is a great need to improve bone health in diabetics using non-pharmaceutical interventions.

Mechanical stimulation associated with exercise and physical activities is long recognized as a potent anabolic factor in promoting bone health [23-25]. The beneficial effects of

mechanical stimulation can be best demonstrated in the stronger bone seen in the accrual of bone mass in the dominant arms of professional tennis players, in contract with the rapid bone loss seen in astronauts and bed-rest patients as their skeletons are deprived from mechanical stimulation [26, 27]. During these bone adaptation processes, osteocytes, the most abundant cells in bone, play a central role. Dispersed in bone matrix and being well-connected with each other as well as the cells lining the bone surfaces, osteocytes serve not only as the primary sensors that detect external mechanical stimuli, but also as a paracrine regulator of osteoblasts and osteoclasts via signaling molecules such as PGE_2, RANKL, OPG and sclerostin/SOST [28-31]. However, the efficacy of applying mechanical stimulation in rescuing diabetic bone diseases is not known and whether diabetic hyperglycemia impairs osteocyte's mechanosensing has yet to be determined.

The objective of the present study was to test the hypothesis that bone's response to anabolic mechanical loading is attenuated in diabetes due to, at least partially, impaired mechanosensing in osteocytes. We first investigated bone's acute responses to exogenously applied ulnar loading in T1D female and male mice as well as their age- and gender-matched normal controls. We then further studied how hyperglycemia associated with severe diabetes affected the responses of osteocytic MLO-Y4 cells to fluid flow stimulation. Our results demonstrated that *in vivo* bone formation was impaired in severe diabetic T1D mouse and hyperglycemia inhibited osteocyte's sensitivity or responses to mechanical stimulation *in vitro*. This study suggests the use of proper glycemic control to restore bone's response to mechanical signals and to improve bone health in diabetic patients.

Methods

In vivo response to ulnar loading

Animals—To test whether hyperglycemia negatively affect *in vivo* bone responses to loading, we used heterozygous C57BL/6-$Ins2^{Akita}$/J (Akita) male and female mice and their age matched wild-type (WT) C57BL/6J controls (7-month-old, N=5-7 mice/group, Jackson Laboratory, Bar Harbor, Maine). Due to the spontaneous Akita mutation that impairs the normal folding and secretion of insulin, Akita male mice develop T1D diabetes at the age of 5 weeks, manifesting severe hyperglycemia, hypoinsulinemia, polydipsia, and polyuria, while Akita females demonstrated milder diabetic symptoms with less severe impairment in β-cell functions [13, 32]. Both Akita females and males were used due to their different stages of disease severity. Fasting blood glucose level was determined using retro-orbital bleeding and a glucometer (OneTouch®, LifeScan, Inc., Milpitas, CA) prior to acute ulnar loading. Body weight was measured at both the beginning and the end of experiments. The animal protocol was approved by the Institutional Animal Care and Use Committee of the University of Delaware.

Ulnar loading experiments—Similar to previous studies [33, 34], we subjected the right forearms of the anaesthetized mice to cyclical compression that induced a peak of ~3500 με near the lateral mid-shaft surface (Fig. 1). Due to different body weight and bone size of each group, the applied load magnitude was determined by strain gauging performed in a separate set of animals (n>=8 ulnae/group). A single-element gauge (EA-06-015DJ-120;

Measurements Group, Inc., Raleigh, NC) was fixed on the relatively flat surface (1-2 mm proximal of the mid-shaft) of the intact ulna attached to the body. The ulna was axially compressed with a gradually increasing load (0.4N/s to 4.2N) using a Bose LM1 TestBench® loading system (Bose Corporation, Framingham, MA), while the strain gauge's output voltage was recorded by LM1's data acquisition unit and converted to strain using a calibrated conversion coefficient [35]. From the strain vs. load curves for the compression tests, the mean compressive rigidity of the ulnae per group was thus calculated. To achieve a consistent 3500 με strain on the ulnar surface, the loading magnitudes for the four groups were calculated to be 2.7±0.5 N, 3±0.4 N, 2.2±0.4N, and 3±0.5N for Akita female, WT females, Akita males and WT males, respectively. Thus, the group averages were chosen to be the applied loading magnitudes, i.e., 2.7 N for Akita females (n=7), 3N for WT females (n=5), 2.2N for Akita males (n=5), and 3N for WT males (n=7). Daily mechanical stimulation was applied at 2Hz, 3 min/day, for 5 consecutive days as published [33]. The mice received dynamic bone labels (calcein 10mg/kg) on Day 4 and Day 15 and were sacrificed on Day 18.

Sample processing and data collection—Both loaded and contralateral non-loaded ulnae were harvested, chemically fixed, embedded in methylmethacrylate, sectioned and polished, and analyzed using an OsteoMeasure® software package and an upright epifluorescent microscope, following the protocols published previously [35, 36]. Static and dynamic histomorphometric measurements were performed on two mid-shaft sections and the average values were used for each animal. For each gender, two types of comparisons were performed. First, the loading effects (loaded ulnae vs. non-loaded ulnae) were tested within the Akita and WT groups with either Student's t tests (for normally distributed data such as bone morphology) or Mann-Whitney U tests (for data without normal distributions). The second type of comparison focused on whether the responses of diabetic Akita mice differed from those of controls. We performed Whitney-Mann U tests on the relative changes, Δ(loaded-nonloaded) data, between the Akita and WT mice. All analyses were performed using Origin (OriginLab, Northampton, MA) with a significance set at $p<0.05$.

In vitro responses to hyperglycemia

Although in vivo bone formation involves osteoblasts, osteocytes, and mesenchymal progenitor cells, we focused our studies on osteocytes, because the inhibitory effects of hyperglycemia on osteoblast proliferation and mineralization have been well established in literature [21, 37, 38]. To test the effects of hyperglycemia on osteocyte mechanosensitivity, we utilized an *in vitro* model where cultured osteocytes were exposed to fluid flow stimulation that mimicked the interstitial fluid flow occurring *in vivo* [39]. Several outcome measures were assessed, such as intracellular Ca^{2+} ($[Ca^{2+}]_i$) peaks, one of the earliest responses of osteocytes to physical stimulation [40-42], and important downstream responses including the secretion of anabolic cytokine (PGE_2), catabolic cytokine (RANKL) and osteocyte apoptosis, which play a role in initiation of bone remodeling [23, 43, 44].

Cells and culture media—MLO-Y4 cells, a generous gift from Dr. Lynda Bonewald (University of Missouri-Kansas City, Kansas City, MO) and a well-characterized model for osteocytes [45], were cultured on type I collagen (BD Biosciences, San Jose, CA, USA)

coated petri-dish. Three culture media were used: i) the regular medium consisted of alpha MEM with 5.5mM D-glucose (Invitrogen Corporation, Carlsbad, CA, USA) supplemented with 5% fetal bovine serum and 5% calf serum (Hyclone Laboratories Inc., Logan, UT, USA); ii) the osmotic control medium consisted of the regular medium described above with the addition of 20 mM L-glucose or 20mM mannitol (Sigma-Aldrich, St. Louis, MO, USA). The total L-glucose concentration (25.5mM, 459mg/dL) corresponded to the averaged fasting blood glucose level in Akita males (detailed in the Results section). iii) the hyperglycemic medium consisted of the regular medium with the addition of 20mM D-glucose (Sigma-Aldrich, St. Louis, MO, USA). The last two media had the same elevated osmolarity, while L-glucose and mannitol, in contrast with D-glucose, cannot be metabolized by cells and thus served as an osmotic control agent [46]. For intracellular calcium imaging, the cells were maintained at 37°C and 5% CO_2 in a humidified incubator for 3, 6, 9, or 12 days, and maintained below 70% confluence. Cells were seeded on type I collagen coated glass slides 24 hours before fluid flow tests. The flow tests were repeated 6-8 times. The number of cells analyzed was 640, 444, and 599 for regular, osmotic control, and hyperglycemic medium, respectively. For downstream responses, the cells were seeded on rat tail type I collagen coated slides at a density of 3000 cells/cm^2 and incubated for 3 days in one of three media described above, prior to fluid flow stimulation.

$[Ca^{2+}]_i$ imaging under fluid flow stimulation—The cells were loaded with 5 μM Fluo-4 Ca^{2+} indicator for 30 min in an incubator followed by three washes with PBS. Slides were then mounted into a parallel plate flow chamber placed on top of an inverted fluorescence microscope (Leica DMI6000) for laminar flow stimulation [41, 47] (Fig. 2A). A unidirectional 2 Pa shear stress was applied to cell surface using a magnetic gear pump (Fig. 2B), and the fluorescence of the cells was recorded with an ORCA-AG interline CCD camera (Hamamatsu, Japan) at 1Hz for 1 min at baseline and 9 min after the onset of the flow (Fig. 2C).

Downstream responses under fluid flow stimulation—Similar to our previous studies [31, 48], osteocytes were exposed to 1 Pa oscillating shear stress at 1Hz for 2 hours in a parallel plate flow chamber with either the normoglycemic control medium, mannitol supplemented osmotic control medium, or hyperglycemic medium. Static control cells were placed inside the parallel chamber for the same time period but without exposure to flow. The cells were then removed from the chamber and incubated at 37°C with a fresh change of either control, hyperglycemic, or mannitol control media. The media and cell lysates were collected after 24 hours of incubation and immediately frozen at -20°C. A sandwich ELISA (R&D Systems, Minneapolis, MN) was used to quantify OPG and RANKL levels in conditioned media. PGE_2 levels were quantified using an EIA kit (Cayman, Ann Arbor, MI). Total protein was determined using a colorimetric kit (Pierce Protein Biology Products, Thermo Fisher Scientific Inc, Rockford, IL) and lysis buffer (Cell Signaling Technology, Danvers, MA). Apoptosis of the cells was measured using a fluorescent Caspase-Glo 3/7 kit (Promega, Madison, WI). Experiments were repeated four times.

Data and statistical analysis—(1) For the analysis of intracellular calcium imaging, the time course of the mean $[Ca^{2+}]_i$ was obtained for each cell using the MetaMorph Imaging

Software (Danaher, Washington, DC). A Ca^{2+} peak was defined as increase in intracellular calcium intensity that was greater than four times that of the baseline standard deviation. The counts of cells exhibiting zero, one, and multiple calcium peaks were obtained for each medium. Chi-Square tests and post-hoc pairwise comparisons using a z-test with Bonferroni adjustment were performed to examine whether the percentages of cells responding with 1+ and 2+ peaks differ among the three media (SAS Institute Inc, Cary, NC). For the responsive cells, the spatiotemporal parameters of the $[Ca^{2+}]_i$ peaks, including the number of peaks, peak magnitude, and the 1st peak response (t_1) and relaxation times (t_2) (Fig. 2C) were analyzed using a customized Matlab program [41, 47]. One way ANOVA with Tukey post hoc tests (OriginLab, Northampton, MA) was used for comparison. The significance level was set at $p<0.05$ for all tests. (2) For the analysis of downstream responses, the protein data from flow stimulated osteocytes were normalized with those from the static control cells. One way ANOVA and Tukey post hoc tests was used for comparison among the three culture media with a $p<0.05$ as described above.

Results

In vivo responses to ulnar loading

Basic metabolic parameters—Akita female mice showed no significant difference in body weight compared with WT mice (25.43±1.40 vs. 26 ±1.87gm), but a 44% elevation in fasting blood glucose level (216.14±35.19 vs. 150.40±6.69 mg/dL, p=0.002) (Table 1). Akita males, however, showed more severe level of diabetes with a 28.5% decrease in body weight (23.40±1.52 vs. 32.71±2.69 gm, p<0.0001) and 227% elevation in fasting blood glucose level (574.80±21.39 vs. 175.57±18.23 mg/dL, p<0.0001, Table 1).

Static bone histomorphometry—For females, after five sessions of ulnar loading, both WT and Akita female mice demonstrated robust bone formation in terms of Ct.B.Ar (+16%, +6.5%) and Ct.Th (+10%, 6.5%) in the loaded ulnae compared with their contralateral non-loaded ulnae (p=0.03, 0.005; and p=0.02, 0.005, respectively, Table 2). The female Akita mice even showed a significant shrink of Ct.Ma.Ar (−12%) after loading (p=0.03, Table 2). Comparing the nonloaded ulnae between the two genotypes, there was no significant difference in tissue total area (Ct.T.Ar), bone area (Ct.B.Ar), marrow area (Ct.Ma.Ar), and cortex thickness (Ct.Th) between Akita and WT females (p=0.2-0.9, Table 2). Regarding the degrees of responses to loading seen in the two genotypes, the change of each of the four static bone indices, Δ(loaded-nonloaded), did not differ significantly (p=0.1-0.6, Table 2). The results, however, were quite different for males. Although WT males showed significant increase in Ct.T.Ar (+10%, p=0.01), Ct.B.Ar (+14%, p=0.0004), and Ct.Th (+11%, p=0.0003) in the loaded ulnae relative to the nonleaded ones, the Akita males did not show any significant change in these parameters under loading (p=0.2-0.7, Table 2). Comparing the non-loaded ulnae between the two genotypes, Akita males showed a significant smaller Ct.B.Ar (−8%, p=0.005) than WT males. Regarding the degrees of responses to loading seen in the two genotypes, the change of the static bone index, Δ(loaded-nonloaded), differed significantly in ΔCt.B.Ar (0.003±0.010 vs. 0.030±0.011 mm^2, p=0.005) and ΔCt.Th (5.4+6.68 vs. 18.34+6.66 μm, p=0.01, Table 2). To better illustrate the dramatic different responses of Akita males and females to mechanical loading, ΔCt.B.Ar was plotted to

clearly demonstrate the robust bone formation in Akita females and greatly attenuated bone formation in Akita males compared with their age- and gender-matched controls, respectively (Fig. 3)

Dynamic bone histomorphometry—The representative images of dynamic bone labeling in the middiaphyseal sections are shown in Fig. 4. For females, mechanical loading significantly increased the bone formation activities on the periosteal surface of the loaded ulnae relative to those of the nonleaded ulnae, in terms of Ps.MS/BS, Ps.MAR, and Ps.BFR/BS for the Akita (p=0.0006-0.005) and the WT (p=0.01, Table 2). Current loading regimen did not significantly influence the dynamic labeling indices on the endosteal surface (where the strains were expected to be lower than the periosteal surface) in the WT females (p=0.06-0.5), while Ec.MS/BS and Ec.MAR were significantly increased in Akita females (p=0.001, 0.0006, Table 2). When comparing the non-loaded ulnae, the Akita female mice even showed a ~2-fold increase in the bone mineralizing surface (MS/BS) at both periosteal and endosteal surfaces (p=0.02, 0.05), while other indices were not significantly different between the two genotypes (Table 2). But overall, the magnitudes of loading effects, as evaluated by the changes of the labeling indices [Δ(loaded-nonloaded)] within the same animals did not differ between WT and Akita females, in agreement with the static histomorphometry data (Table 2). However, a different pattern was found in males. As expected, the WT males showed increases in all the labeling indices in the periosteal surface (Ps.MS/BS, Ps.MAR, Ps.BFR/BS) and bone formation rate (Ec.BFR/BS) in the endosteal surface (p=0.001-0.05). While the Akita males showed activation of bone formation in terms of Ps.MS/BS, Ec.MS/BS, Ec.MAR, and Ec.BFR/BS (p=0.008-0.05) relative to the non-loaded ulnae, they failed to increase Ps.MAR and Ps.BFR/BS in the periosteum (p=1, Table 2) and to induce significant changes in the static indices (Ct.T.Ar, Ct.B.Ar, Ct.Ma.Ar, & Ct.Th, p=0.2-07, Table 2). Furthermore, the Akita males showed reductions in the relative changes of Δ(loaded-nonloaded) in terms of Ct.B.Ar (0.003±0.010 vs. 0.030±0.011mm^2, p=0.005), Ct.Th (5.30±6.68 vs. 18.34±6.66μm, p=0.01), as well as periosteal bone formation rate (Ps.BFR/BS, p=0.02). For the non-loaded ulnae, in contrast to the 2-fold increase in MS/BS found in Akita females, Akita males even demonstrated 30%, and 70% decrease in the MS/BS in the periosteal and endosteal surfaces, respectively (Table 2). Overall, the Akita males demonstrated diminished anabolic responses compared with WT males.

In vitro responses to hyperglycemia

$[Ca^{2+}]_i$ imaging under fluid flow stimulation—Because no significant differences were observed in $[Ca^{2+}]_i$ parameters among the various culture times (data not shown), the data were pooled for analysis. Our results (Fig. 5) demonstrated that hyperglycemia impaired MLO-Y4 mechanosensitivity to fluid flow due to the elevated osmolarity and glucose-specific effects. Although the percentage of responding osteocytes with at least one calcium peak did not differ among the three culture conditions (Fig. 5A), the cell populations capable of releasing multiple peaks were significantly reduced under hyperglycemia conditions (Fig. 5B). This particular effect was likely due to presence of D-glucose because the increase of osmolarity in the L-glucose control medium did not show this effect. However, elevated medium osmolarity did suppress cell's average peak number and the response time to the 1st

peak (Figs.5C, 5E). The peak magnitude and relaxation time were not altered in the three culture conditions (Figs. 5D, 5F).

Downstream responses under fluid flow stimulation—Osteocytes in the normoglycemic control or mannitol-supplemented media showed decreased Caspase 3/7 level under fluid flow compared with those in static (no fluid flow) controls and this beneficial effect of fluid flow was abolished in the hyperglycemic group (Fig. 6A). Similarly, fluid flow resulted in decreased secretion of sRANKL by osteocytes under the normoglycemic and osmotic control media, which was reversed in the hyperglycemic medium (Fig. 6B). The OPG secretion was too low to be detected in our system and thus not reported here. The release of PGE_2 was increased in osteocytes by fluid flow stimulation under the normoglycemic and osmotic control media, which was suppressed in the hyperglycemic medium (Fig. 6C).

Discussion

Our in vivo ulnar loading study, for the first time, revealed that untreated severe type 1 diabetic bone showed much reduced responses to anabolic mechanical loading in contrast to the normoglycemic controls. This important finding implies that proper diabetic control may be essential to maximize the beneficial effects of exercise on skeletal health. As expected, the normoglycemic WT males and females both responded to the current loading regimen (~3500με, 2Hz, 3 min/day for 5 days) with robust bone formation in their loaded ulnae compared with nonleaded contralateral ulnae. Female Akita mice, with a mild elevation in the fasting blood glucose levels (+44%) and normal body weights, responded to the loading stimulus as well as the WT controls with no significant difference in the changes of static and dynamic indices (Δ(loaded-nonloaded), p=0.1-0.8, Table 2, and Fig. 3). In contrast, the Akita males with extremely higher glucose levels (+227%) and lower body weights (−28.5%) showed attenuated bone formation compared with WT males (Table 2 and Fig. 3). More severe diabetic symptoms were present in Akita males as found in previous studies [49, 50], which was in agreement with that Akita males had more pronounced reduction in both pancreatic beta-cell functions and serum insulin level [32]. Compared with age- and gender-matched controls, the plasma insulin level in Akita males showed a two-fold decrease at the age of 8 weeks and the pancreatic insulin content exhibited a dramatic 10-fold decrease at the age of 22 weeks [50]. This severe diabetic phenotype in the Akita males may account for the diminished anabolic response to ulnar loading, as shown in the significant reduction in the change of load-induced bone area ($0.003 mm^2$ vs. $0.030 mm^2$, p=0.005, Fig. 3). This lack of response was mainly due to the suppression of periosteal bone apposition (ΔPs.BFR/BS, p=0.02, Table 2).

The different loading responses of Akita males and females were unlikely due to the sex hormones, despite of their known influence on bone growth [51, 52]. Bone's response to mechanical loading does not appear to be gender-dependent [53], at least under the acute loading regimen employed in this study, where both male and female WT mice showed similar changes of static and dynamic indices (Δ(loaded-nonloaded), Table 2). To account for the baseline difference among the male/female and normal/diabetic groups, we used the nonloaded contralateral ulna as internal control for each animal and compared the relative

changes reflecting the responses to loading. Furthermore, bone formation rate was reported as normalized value in reference to the bone surface (BFR/BS). These considerations and the *in vivo* results reported herein lead to the conclusion that bone's response to acute anabolic mechanical loading is attenuated in diabetic mice with severe hyperglycemia. The inhibitory effects of hyperglycemia on osteoblast proliferation and mineralization [21, 37, 38] might be accounted for our in vivo results. However, the contribution of osteocytes that are responsible for sensing mechanical stimuli [54] remained unclear until the present study.

Our in vitro studies demonstrated that even a short-term (up to 12 days) hyperglycemia treatment with D-glucose (459 mg/dL) impaired osteocyte's intracellular calcium signaling. We focused on intracellular calcium as an outcome in our study because it is one of the earliest cellular responses to physical stimuli in bone cells. As summarized in previous reviews [23, 39], upon mechanical stimulation, intracellular calcium responses are initiated within seconds, followed by the release of ATP [34, 55], nitric oxide [56, 57], and PGE_2 [58, 59] within minutes or hours, leading to long-term changes in signaling molecules such as sclerostin [28], DMP1 [60, 61], and RANKL/OPG [31]. These signaling molecules could act on neighboring osteocytes as well as osteoblasts and osteoclasts on the bone surfaces in both autocrine and paracrine fashions [54]. Our *in vitro* study demonstrated that 3-12 days culture in hyperglycemia significantly reduced osteocytes' ability in releasing repetitive calcium peaks under fluid flow stimulation (Fig. 5). This robust, repetitive calcium signaling has been identified as a unique feature of osteocytes, which is directly related to the calcium wave propagation among osteocytes and plays a significant role in intercellular communication [41] during bone adaptation processes. Moreover, we demonstrated that osteocyte's downstream responses to fluid flow, including activation of anti-apoptotic pathways, suppression of catabolic factor RANKL (activation of osteoclast function), and increased anabolic PGE2 release, were significantly attenuated/abolished under hyperglycemia (25mM D-glucose, Fig. 6). These negative effects were mainly due to the elevation of glucose level but not the associated increase in osmolarity in the hyperglycemic medium, because the mannitol-supplemented medium with elevated osmolarity did not show such negative effects (Fig. 6).

Data from this study support the clinical practice of proper glycemic control in diabetes care. Besides the benefits on cardiovascular and microcirculation system, normalizing the blood glucose level can potentially improve bone health and reduce fracture risks through i) overcoming the negative effects of hyperglycemia identified previously on bone progenitor cells [19], osteoblast's functions [20, 21], and composition of bone matrix [8, 9, 15], and ii) improving osteocyte's sensitivity and the overall anabolic response to mechanical stimulation. Because physical activities are strongly recommended for diabetic patients (see guidelines in the CDC website), the present study suggests that the exercise's benefits on skeletal system could be maximized when the functions of osteoblasts and osteoclasts are better regulated by osteocytes under normoglycemia. However, not all anti-hyperglycemia medications are found to be beneficial for bone health. Recent large clinical data showed negative bone effects associated with long-term use of hiazolidinediones [11, 22]. The present study adopted the phenotypically different Akita male and female mice with

differential endogenous insulin levels (discussed below) and the results suggest the profound effects of insulin deficiency on the skeletal system.

Insulin inserts profound impact on bone growth and properties. Decreased insulin secretion in Akita mice has been well established in literature. Yoshioka et al. (1997) reported that, at the age of 7-weeks, the immunoreactive insulin levels in plasma (pmol/l) were, significantly lower in diabetic mice than in unaffected mice: 193±51 for diabetic males and 471±73 for unaffected males; 248±82 for diabetic females and 379±78 for unaffected females (n=10/group) [32]. Later studies confirmed the dramatic decreases in plasma insulin level and the total insulin produced in pancreas of male mice compared with normal control mice [50]. With the progression of age from 4 to 30 weeks (similar to the age of the mice used in this study), diabetic Akita males showed significant decreases in the relative areas of immunologically detectable insulin from 20.7% to 9.1% (4 vs. 30 weeks), while they were maintained in Akita females (45.9% to 49.6%, [32]). Based on these data and their agreement with our recorded blood glucose levels (Table 1), the female Akita mice in our study were anticipated to have higher insulin level and better beta-cell function than the Akita males, which may partially contribute to the relatively normal phenotype (in terms of body weight, bone size and bone stiffness) observed in the Akita female mice. This is also in agreement with a recent study finding that exogenous insulin treatment rescued the degradation of bone mechanical properties and deficiency in bone growth in 12-week-old streptozotocin-induced diabetic rats during eight weeks of experiments [62]. The anabolic effects observed in our WT and Akita female mice might be due to the anabolic effects of endogenous insulin on osteoblasts through ERK activation and cyclooxygenase-2 expression [63], and/or its anti-hyperglycemic effects on osteocytes' mechanosensing as discussed earlier. It will be interesting to further test whether exogenous insulin treatment will restore diabetic bone's response to mechanical loading in the Akita diabetic model.

There are several limitations on this study. Firstly, since diabetes is a chronic metabolic disease, many factors may be involved in the changes of the skeletal system in diabetics. We focused on hyperglycemia in the present investigations, because, as the most obvious marker for diabetes, hyperglycemia has shown negative effects on other bone cells [20, 21]. Other factors such as accumulated advanced glycation end products [8, 19], insulin deficiency [64], oxidative stress, and chronic inflammation [17, 18] may also be responsible for the diabetic disorders observed herein and warranted for further investigations. The other limitation was the relative small sample size (n=5-7) used in the in vivo experiments. A larger sample size may help detect the more subtle alterations, if any, in Akita female mice. Another limitation was the use of Akita female and male mice representing different severity levels in diabetes and the associated hyperglycemia. It would be better to test the effects of varied diabetes/hyperglycemia levels within the same genders and compare with the age-matched normal controls. We also note that the loading regimen adopted in the present study represents short-term (5 days) and high intensity (3500 με) loading, while the exercise regimens prescribed to patients may vary in intensity and duration. A range of physiological loading/exercise parameters should be tested *in vivo*. Furthermore, the outcomes measured in the study were limited to bone histomorphometry and intracellular calcium signaling, more comprehensive studies on the protein and gene expression in diabetic bones subjected

to mechanical stimulations should be performed in the future [65]. Lastly, although the Akita mouse in our *in vivo* studies is a well-established T1D model, the majority of diabetic patients are T2D. We are planning to repeat the *in vivo* loading studies using high-fat-diet induced T2D model as established in literature [66, 67].

Despite these limitations, the current studies, for the first time, demonstrated that diabetic bone can respond to mechanical loading when the hyperglycemia is not severe, suggesting that mechanical interventions may be useful to improve bone health and reduce fracture risk in mildly affected diabetic patients, and proper glycemic control may help maximize the beneficial effects of exercise on diabetic skeleton.

Acknowledgments

The authors thank Dr. Ryan Pohlig in the college of Health Sciences of University of Delaware for his advice on statistical analysis in this study. The study was supported by the following funds: NIH AR054385 (LW), NIH P30GM103333 (LW), DOD PR120788 (XLL) and NSERC 341704 (LY).

References

1. Janghorbani M, et al. Systematic review of type 1 and type 2 diabetes mellitus and risk of fracture. Am J Epidemiol. 2007; 166(5):495–505. [PubMed: 17575306]
2. Vestergaard P. Discrepancies in bone mineral density and fracture risk in patients with type 1 and type 2 diabetes--a meta-analysis. Osteoporos Int. 2007; 18(4):427–44. [PubMed: 17068657]
3. Kenzora JE, et al. Hip fracture mortality. Relation to age, treatment, preoperative illness, time of surgery, and complications. Clin Orthop Relat Res. 1984; (186):45–56. [PubMed: 6723159]
4. Borrelli J Jr. et al. Physiological challenges of bone repair. J Orthop Trauma. 2012; 26(12):708–11. [PubMed: 23047710]
5. Bechtold S, et al. Bone size normalizes with age in children and adolescents with type 1 diabetes. Diabetes Care. 2007; 30(8):2046–50. [PubMed: 17456838]
6. Nyman JS, et al. Increasing duration of type 1 diabetes perturbs the strength-structure relationship and increases brittleness of bone. Bone. 2011; 48(4):733–40. [PubMed: 21185416]
7. Saha MT, et al. Bone mass and structure in adolescents with type 1 diabetes compared to healthy peers. Osteoporos Int. 2009; 20(8):1401–6. [PubMed: 19083073]
8. Saito M, et al. Role of collagen enzymatic and glycation induced cross-links as a determinant of bone quality in spontaneously diabetic WBN/Kob rats. Osteoporos Int. 2006; 17(10):1514–23. [PubMed: 16770520]
9. Rosenbloom AL, Silverstein JH. Connective tissue and joint disease in diabetes mellitus. Endocrinol Metab Clin North Am. 1996; 25(2):473–83. [PubMed: 8799711]
10. Burghardt AJ, et al. High-resolution peripheral quantitative computed tomographic imaging of cortical and trabecular bone microarchitecture in patients with type 2 diabetes mellitus. J Clin Endocrinol Metab. 2010; 95(11):5045–55. [PubMed: 20719835]
11. Patsch JM, et al. Increased cortical porosity in type 2 diabetic postmenopausal women with fragility fractures. J Bone Miner Res. 2013; 28(2):313–24. [PubMed: 22991256]
12. Melton LJ 3rd, et al. A bone structural basis for fracture risk in diabetes. J Clin Endocrinol Metab. 2008; 93(12):4804–9. [PubMed: 18796521]
13. Coe LM, Zhang J, McCabe LR. Both spontaneous Ins2(+/−) and streptozotocin-induced type I diabetes cause bone loss in young mice. J Cell Physiol. 2012; 228(4):689–95. [PubMed: 22886636]
14. Reinwald S, et al. Skeletal changes associated with the onset of type 2 diabetes in the ZDF and ZDSD rodent models. Am J Physiol Endocrinol Metab. 2009; 296(4):E765–74. [PubMed: 19158319]

15. Silva MJ, et al. Type 1 diabetes in young rats leads to progressive trabecular bone loss, cessation of cortical bone growth, and diminished whole bone strength and fatigue life. J Bone Miner Res. 2009; 24(9):1618–27. [PubMed: 19338453]
16. Kawashima Y, et al. Type 2 diabetic mice demonstrate slender long bones with increased fragility secondary to increased osteoclastogenesis. Bone. 2009; 44(4):648–55. [PubMed: 19150422]
17. McCabe L, Zhang J, Raehtz S. Understanding the skeletal pathology of type 1 and 2 diabetes mellitus. Crit Rev Eukaryot Gene Expr. 2011; 21(2):187–206. [PubMed: 22077156]
18. McCabe LR. Understanding the pathology and mechanisms of type I diabetic bone loss. J Cell Biochem. 2007; 102(6):1343–57. [PubMed: 17975793]
19. McCarthy AD, et al. Effects of advanced glycation end-products on the proliferation and differentiation of osteoblast-like cells. Mol Cell Biochem. 1997; 170(1-2):43–51. [PubMed: 9144317]
20. Bouillon R, et al. Influence of age, sex, and insulin on osteoblast function: osteoblast dysfunction in diabetes mellitus. J Clin Endocrinol Metab. 1995; 80(4):1194–202. [PubMed: 7714089]
21. Botolin S, McCabe LR. Chronic hyperglycemia modulates osteoblast gene expression through osmotic and non-osmotic pathways. J Cell Biochem. 2006; 99(2):411–24. [PubMed: 16619259]
22. Yaturu S. Diabetes and skeletal health. J Diabetes. 2009; 1(4):246–54. [PubMed: 20923525]
23. Duncan RL, Turner CH. Mechanotransduction and the functional response of bone to mechanical strain. Calcif Tissue Int. 1995; 57(5):344–58. [PubMed: 8564797]
24. Forwood MR, Burr DB. Physical activity and bone mass: exercises in futility? Bone Miner. 1993; 21(2):89–112. [PubMed: 8358253]
25. Mosley JR, Lanyon LE. Strain rate as a controlling influence on adaptive modeling in response to dynamic loading of the ulna in growing male rats. Bone. 1998; 23(4):313–8. [PubMed: 9763142]
26. Leblanc AD, et al. Bone mineral loss and recovery after 17 weeks of bed rest. J Bone Miner Res. 1990; 5(8):843–50. [PubMed: 2239368]
27. Sibonga JD, et al. Recovery of spaceflight-induced bone loss: bone mineral density after long-duration missions as fitted with an exponential function. Bone. 2007; 41(6):973–8. [PubMed: 17931994]
28. Robling AG, et al. Mechanical stimulation of bone in vivo reduces osteocyte expression of Sost/sclerostin. J Biol Chem. 2008; 283(9):5866–75. [PubMed: 18089564]
29. Tatsumi S, et al. Targeted ablation of osteocytes induces osteoporosis with defective mechanotransduction. Cell Metab. 2007; 5(6):464–75. [PubMed: 17550781]
30. Weinbaum S, Cowin SC, Zeng Y. A model for the excitation of osteocytes by mechanical loading-induced bone fluid shear stresses. J Biomech. 1994; 27(3):339–60. [PubMed: 8051194]
31. You L, et al. Osteocytes as mechanosensors in the inhibition of bone resorption due to mechanical loading. Bone. 2008; 42(1):172–9. [PubMed: 17997378]
32. Yoshioka M, et al. A novel locus, Mody4, distal to D7Mit189 on chromosome 7 determines early-onset NIDDM in nonobese C57BL/6 (Akita) mutant mice. Diabetes. 1997; 46(5):887–94. [PubMed: 9133560]
33. Robling AG, et al. Modulation of appositional and longitudinal bone growth in the rat ulna by applied static and dynamic force. Bone. 2001; 29(2):105–13. [PubMed: 11502470]
34. Li J, et al. The P2X7 nucleotide receptor mediates skeletal mechanotransduction. J Biol Chem. 2005; 280(52):42952–9. [PubMed: 16269410]
35. Robling AG, Turner CH. Mechanotransduction in bone: genetic effects on mechanosensitivity in mice. Bone. 2002; 31(5):562–9. [PubMed: 12477569]
36. Hillam RA, Skerry TM. Inhibition of bone resorption and stimulation of formation by mechanical loading of the modeling rat ulna in vivo. J Bone Miner Res. 1995; 10(5):683–9. [PubMed: 7639102]
37. Gopalakrishnan V, et al. Effects of glucose and its modulation by insulin and estradiol on BMSC differentiation into osteoblastic lineages. Biochem Cell Biol. 2006; 84(1):93–101. [PubMed: 16462893]
38. Balint E, et al. Glucose-induced inhibition of in vitro bone mineralization. Bone. 2001; 28(1):21–8. [PubMed: 11165939]

39. Klein-Nulend J, et al. Mechanosensation and transduction in osteocytes. Bone. 2013; 54(2):182–90. [PubMed: 23085083]
40. Hung CT, et al. Intracellular Ca2+ stores and extracellular Ca2+ are required in the real-time Ca2+ response of bone cells experiencing fluid flow. J Biomech. 1996; 29(11):1411–7. [PubMed: 8894921]
41. Lu XL, et al. Osteocytic network is more responsive in calcium signaling than osteoblastic network under fluid flow. J Bone Miner Res. 2012; 27(3):563–74. [PubMed: 22113822]
42. Lu XL, et al. Calcium response in osteocytic networks under steady and oscillatory fluid flow. Bone. 2012; 51(3):466–73. [PubMed: 22750013]
43. Verborgt O, et al. Spatial distribution of Bax and Bcl-2 in osteocytes after bone fatigue: complementary roles in bone remodeling regulation? J Bone Miner Res. 2002; 17(5):907–14. [PubMed: 12009022]
44. Kim CH, et al. Oscillatory fluid flow-induced shear stress decreases osteoclastogenesis through RANKL and OPG signaling. Bone. 2006; 39(5):1043–7. [PubMed: 16860618]
45. Bonewald LF. Establishment and characterization of an osteocyte-like cell line, MLO-Y4. J Bone Miner Metab. 1999; 17(1):61–5. [PubMed: 10084404]
46. El-Remessy AB, et al. High glucose-induced tyrosine nitration in endothelial cells: role of eNOS uncoupling and aldose reductase activation. Invest Ophthalmol Vis Sci. 2003; 44(7):3135–43. [PubMed: 12824263]
47. Huo B, et al. Fluid Flow Induced Calcium Response in Bone Cell Network. Cell Mol Bioeng. 2008; 1(1):58–66. [PubMed: 20852730]
48. Cheung WY, Simmons CA, You L. Osteocyte apoptosis regulates osteoclast precursor adhesion via osteocytic IL-6 secretion and endothelial ICAM-1 expression. Bone. 2012; 50(1):104–10. [PubMed: 21986000]
49. Umino Y, Solessio E. Loss of scotopic contrast sensitivity in the optomotor response of diabetic mice. Invest Ophthalmol Vis Sci. 2013; 54(2):1536–43. [PubMed: 23287790]
50. Naito M, et al. Therapeutic impact of leptin on diabetes, diabetic complications, and longevity in insulin-deficient diabetic mice. Diabetes. 2011; 60(9):2265–73. [PubMed: 21810600]
51. Neu CM, et al. Bone densities and bone size at the distal radius in healthy children and adolescents: a study using peripheral quantitative computed tomography. Bone. 2001; 28(2):227–32. [PubMed: 11182383]
52. Gilsanz V, et al. Gender differences in vertebral body sizes in children and adolescents. Radiology. 1994; 190(3):673–7. [PubMed: 8115609]
53. Lynch ME, et al. Cancellous bone adaptation to tibial compression is not sex dependent in growing mice. J Appl Physiol (1985). 2010; 109(3):685–91. [PubMed: 20576844]
54. Bonewald LF. The amazing osteocyte. J Bone Miner Res. 2011; 26(2):229–38. [PubMed: 21254230]
55. Genetos DC, et al. Oscillating fluid flow activation of gap junction hemichannels induces ATP release from MLO-Y4 osteocytes. J Cell Physiol. 2007; 212(1):207–14. [PubMed: 17301958]
56. Zaman G, et al. Mechanical strain stimulates nitric oxide production by rapid activation of endothelial nitric oxide synthase in osteocytes. J Bone Miner Res. 1999; 14(7):1123–31. [PubMed: 10404012]
57. Vatsa A, Smit TH, Klein-Nulend J. Extracellular NO signalling from a mechanically stimulated osteocyte. J Biomech. 2007; 40(Suppl 1):S89–95. [PubMed: 17512530]
58. Klein-Nulend J, et al. Pulsating fluid flow stimulates prostaglandin release and inducible prostaglandin G/H synthase mRNA expression in primary mouse bone cells. J Bone Miner Res. 1997; 12(1):45–51. [PubMed: 9240724]
59. Ajubi NE, et al. Pulsating fluid flow increases prostaglandin production by cultured chicken osteocytes--a cytoskeleton-dependent process. Biochem Biophys Res Commun. 1996; 225(1):62–8. [PubMed: 8769095]
60. Gluhak-Heinrich J, et al. Mechanical loading stimulates dentin matrix protein 1 (DMP1) expression in osteocytes in vivo. J Bone Miner Res. 2003; 18(5):807–17. [PubMed: 12733719]

61. Yang W, et al. Dentin matrix protein 1 gene cis-regulation: use in osteocytes to characterize local responses to mechanical loading in vitro and in vivo. J Biol Chem. 2005; 280(21):20680–90. [PubMed: 15728181]

62. Erdal N, et al. The effect of insulin therapy on biomechanical deterioration of bone in streptozotocin (STZ)-induced type 1 diabetes mellitus in rats. Diabetes Res Clin Pract. 2012; 97(3):461–7. [PubMed: 22483749]

63. Zhong X, Wang H, Jian X. Insulin augments mechanical strain-induced ERK activation and cyclooxygenase-2 expression in MG63 cells through integrins. Exp Ther Med. 2014; 7(1):295–299. [PubMed: 24348809]

64. Donath MY, et al. Inflammatory mediators and islet beta-cell failure: a link between type 1 and type 2 diabetes. J Mol Med (Berl). 2003; 81(8):455–70. [PubMed: 12879149]

65. Mantila Roosa SM, Liu Y, Turner CH. Gene expression patterns in bone following mechanical loading. J Bone Miner Res. 2012; 26(1):100–12. [PubMed: 20658561]

66. Ionova-Martin SS, et al. Changes in cortical bone response to high-fat diet from adolescence to adulthood in mice. Osteoporos Int. 2011; 22(8):2283–93. [PubMed: 20941479]

67. Zernicke RF, et al. Long-term, high-fat-sucrose diet alters rat femoral neck and vertebral morphology, bone mineral content, and mechanical properties. Bone. 1995; 16(1):25–31. [PubMed: 7742079]

Highlights

- We aimed to test whether mechanical loading, a potent anabolic factor, can rescue the weak bone phenotype in diabetics
- Akita female mice with mild diabetes responded to anabolic ulnar loading, while Akita males with severe hyperglycemia showed diminished responses
- Hyperglycemia impaired MLO-Y4 osteocyte's responses to fluid flow stimulation (intracellular calcium, apoptosis, RANKL, and PGE_2 release).
- Failure to maintain normal glucose levels may impair bone's responses to mechanical loading in diabetics

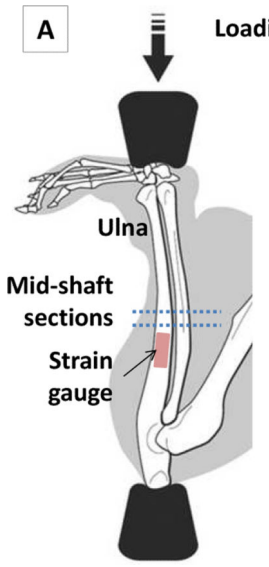

B

	7	2.7N
	5	3.0N
	5	2.2N
	7	3.0N

Fig. 1.

(**A**) In vivo ulnar loading model. Peak strain was validated using strain gauges placed on the relative flat area (1-2mm proximal of the mid-shaft). Induced bone formation was evaluated in the cross-sections of the mid-shaft (dotted lines). (**B**) Calibrated peak load magnitudes to achieve similar 3500 με surface strain in the four experimental groups.

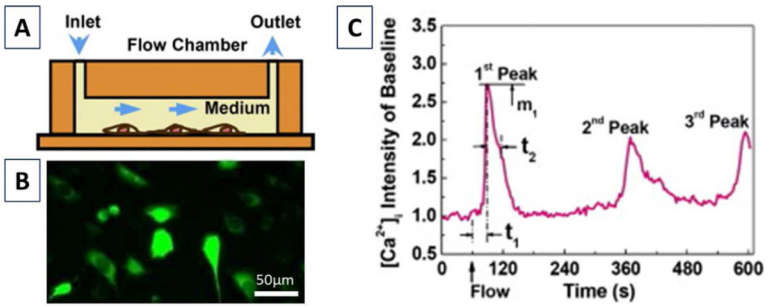

Fig. 2.

Intracellular calcium imaging. **(A)** Osteocytes were exposed to fluid flow stimulation in a laminar flow chamber. **(B)** Osteocytes were dyed with Fluo-4 and imaged for 10 min. **(C)** A representative calcium response and the quantified spatiotemporal parameters (number of peaks, 1^{st} peak magnitude (m_1), 1^{st} peak response time (t_1) and relaxation time (t_2)).

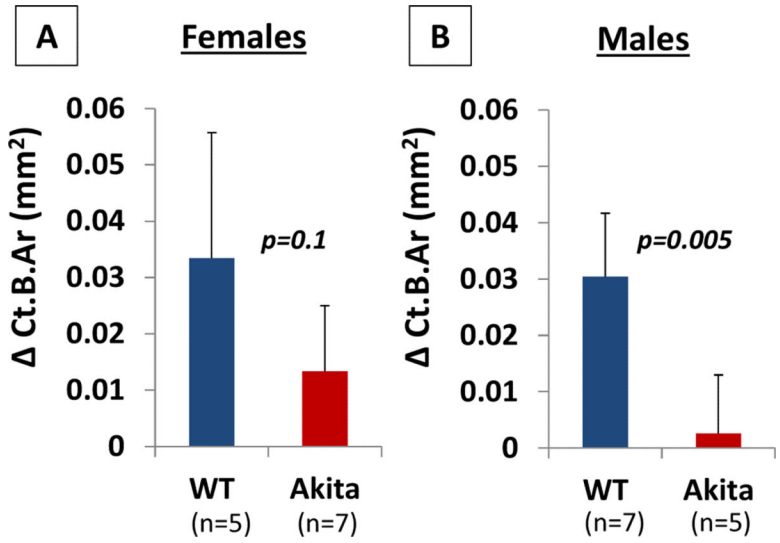

Fig. 3.

Load-induced changes in bone area. **(A)** Females Akita with mild hyperglycemia showed similar bone formation as WT; **(B)** The effect of loading was completely abolished in Akita males with severe hyperglycemia. The p values were for Mann-Whitney U tests. Data are presented as mean ±SD.

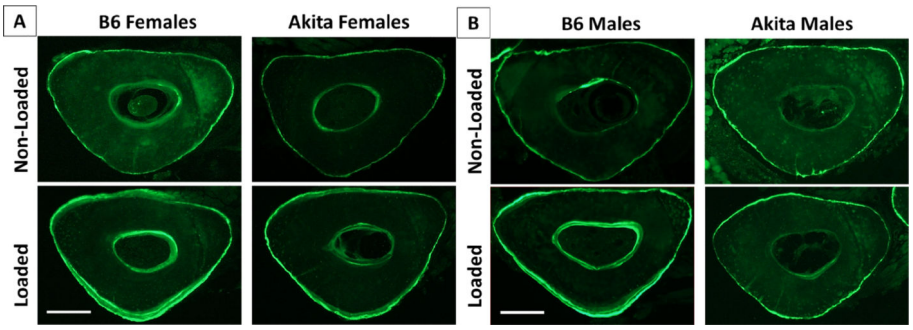

Fig. 4.

Representative cross-section images showing bone labels for **(A)** normal and Akita females and (**B**) normal and Akita males. Bar=0.2mm.

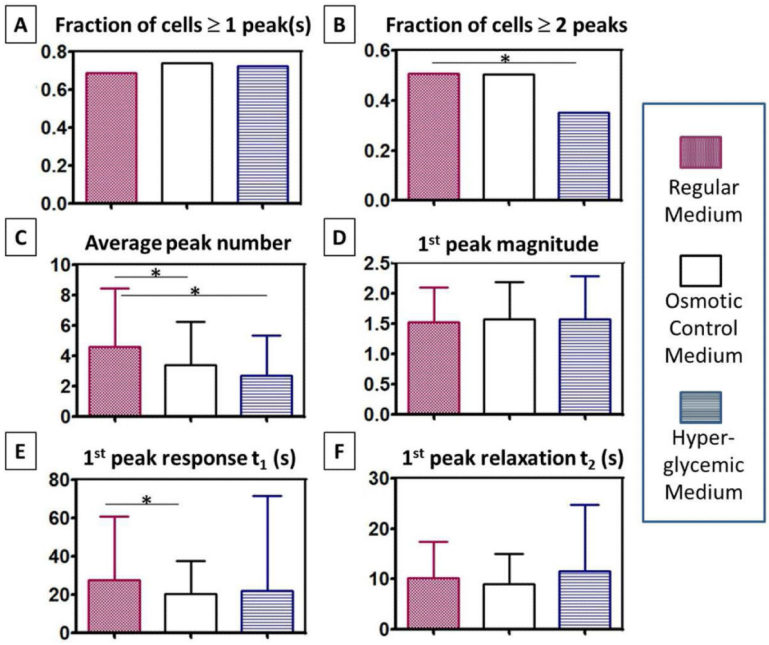

Fig. 5.

Hyperglycemia impaired osteocytes' multiple $[Ca^{2+}]_i$ responses to fluid flow. (**A**) No significance among three groups on the fraction of cells responding with one peak or more; (**B**) Significant decrease in the fraction of cells responding with multiple peaks in the hyperglycemic medium (35%) versus regular (51%) and osmotic control media (50%). (**C**) The average peak number decreased in media with elevated osmolarity. (**D**) No difference in the 1st peak magnitude. (**E**) Faster responding time from the onset of flow to the 1st peak in the osmotic control medium. (F) No difference in the relaxation time from the 1st peak to baseline. Regular medium contained 5.5mM D-glucose, while the osmotic control medium and hyperglycemic medium contained additional 20mM L-glucose, and 20mM D-glucose, respectively. The flow tests were repeated 6-8 times with 444-640 cells analyzed per medium condition. * $p<0.05$. Bars indicate one standard deviation.

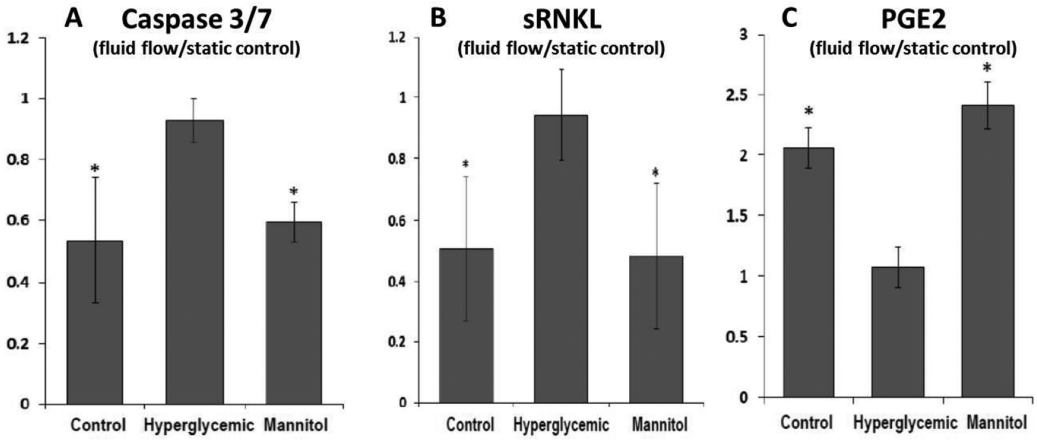

Fig. 6.

Hyperglycemia impaired osteocyte's downstream responses to fluid flow. (**A**) Caspase 3/7 expression; (**B**) Soluble RANKL expression; (**C**) PGE2 concentration in media. Data were normalized to those under static no-flow condition. All tests were repeated 4 times. * indicated $p<0.05$ vs. hyperglycemic condition (ANOVA with post hoc Tukey tests). Bars indicate one standard deviation.

Table 1

Basic metabolic data

Groups	C57BL/6J Females	Akita Het Females	C57BL/6J Males	Akita Het Males
Sample size N	5	7	7	5
Age at Day 1 of experiment (weeks)	29	29	29	29
BW at Day 1 of experiment (g)	26±1.87	25.43±1.40	32.71 ±2.69	23.40±1.52*
BW at Day 18 of experiment (g)	24.60±2.95	24.71±1.60	31.51±2.10	23.40±0.89*
Fasting blood glucose level (mg/dL)	150.40±6.69	216.14±35.19*	175.57±18.23	574.80±21.39*

Note:

*p<0.05 vs. WT controls of the same gender (Student t tests). Data are presented as mean ± standard deviation.

Table 2

Static and Dynamic Histomorphometric Results of Ulnar Loading on Non-Diabetic Akita Male and Female Mice

Female Data	WT Females (n=5)			Akita Females (n=7)			p Values or Pairwise Comparisons			
	nonloaded	loaded	Δ (loaded-nonloaded)	nonloaded	loaded	Δ (loaded-nonloaded)	WT Females (loaded vs. nonloaded)	Akita Females (loaded vs. nonloaded)	nonloaded ulnae (Akita vs. WT)	Δ (loaded-nonloaded) (Akita vs. WT)
Ct.T.Ar (mm^2)	0.255 (0.010)	0.289 (0.019)	0.034 (0.028)	0.257 (0.023)	0.266 (0.021)	0.008 (0.015)	**0.05**	0.2	0.9	0.6
Ct.B.Ar (mm^2)	0.218 (0.007)	0.252 (0.016)	0.033 (0.022)	0.215 (0.014)	0.229 (0.010)	0.013 (0.012)	**0.03**	**0.02**	0.7	0.1
Ct.Ma.Ar (mm^2)	0.369 (0.004)	0.037 (0.004)	0.0006 (0.007)	0.042 (0.011)	0.037 (0.013)	−0.005 (0.005)	0.9	**0.03**	0.4	0.4
Ct.Th (μm)	160.17 (4.10)	176.04 (4.80)	15.87 (6.19)	156.34 (5.25)	166.57 (8.51)	10.23 (6.31)	**0.005**	**0.005**	0.2	0.1
Ps.MS/BS (%)	12.55 (5.30)	36.60 (5.43)	24.05 (8.83)	20.02 (3.03)	49.83 (8.86)	29.81 (7.14)	**0.01**	**0.0006**	**0.02**	0.3
Ps.MAR (μm/day)	0 (0)	0.942 (0.506)	0.942 (0.506)	0.050 (0.133)	0.668 (0.396)	0.617 (0.396)	**0.01**	**0.009**	1	0.3
Ps.BFR/BS ($\mu m^3/\mu m^2$/day)	0 (0)	0.364 (0.221)	0.364 (0.221)	0.013 (0.036)	0.362 (0.226)	0.348 (0.222)	**0.01**	**0.005**	1	0.8
Ec.MS/BS (%)	9.51 (3.77)	16.91 (5.90)	7.40 (5.00)	17.06 (7.88)	43.96 (10.93)	26.90 (17.33)	0.06	**0.001**	**0.05**	0.1
Ec.MAR (μm/day)	0.155 (0.215)	0.0670 (1.011)	0.540 (0.909)	0.428 (0.380)	0.789 (0.324)	0.361 (0.426)	0.5	0.2	0.2	0.8
Ec.BFR/BS ($\mu m^3/\mu m^2$/day)	0.024 (0.037)	0.129 (0.186)	0.104 (0.160)	0.090 (0.083)	0.393 (0.200)	0.303 (0.230)	0.5	**0.0006**	0.1	0.1

Male Data	WT Males (n=7)			Akita Males (n=5)			p Values of Pairwise Comparisons			
	nonloaded	loaded	Δ (loaded-nonloaded)	nonloaded	loaded	Δ (loaded-nonloaded)	WT Males (loaded vs. nonloaded)	Akita Males (loaded vs. nonloaded)	nonloaded ulnae (Akita vs. WT)	Δ (loaded-nonloaded) (Akita vs. WT)
Ct.T.Ar (mm^2)	0.258 (0.012)	0.285 (0.009)	0.027 (0.017)	0.245 (0.013)	0.242 (0.013)	−0.002 (0.015)	**0.01**	0.7	0.1	1
Ct.B.Ar (mm^2)	0.220 (0.008)	0.250 (0.008)	0.030 (0.011)	0.203 (0.008)	0.205 (0.004)	0.003 (0.010)	**0.0004**	0.6	**0.005**	**0.005**
Ct.Ma.Ar (mm^2)	0.038 (0.007)	0.035 (0.008)	−0.003 (0.008)	0.042 (0.012)	0.037 (0.011)	−0.005 (0.006)	0.3	0.2	0.5	0.3
Ct.Th (μm)	158.16 (5.80)	176.49 (10.15)	18.34 (6.66)	147.49 (8.83)	152.79 (11.37)	5.30 (6.68)	**0.0003**	0.2	0.2	**0.01**
Ps.MS/BS (%)	22.02 (9.28)	52.77 (18.82)	30.75 (23.01)	14.45 (1.67)	31.69 (6.86)	17.24 (7.55)	**0.001**	**0.008**	0.1	0.4
Ps.MAR (μm/day)	0.290 (0.502)	1.001 (0.616)	0.711 (0.740)	0.135 (0.303)	0.064 (0.144)	−0.071 (0.366)	**0.04**	1	0.6	0.07
Ps.BFR/BS ($\mu m^3/\mu m^2$/day)	0.098 (0.151)	0.642 (0.571)	0.544 (0.608)	0.025 (0.055)	0.028 (0.064)	0.004 (0.094)	**0.02**	1	0.6	**0.02**
Ec.MS/BS (%)	7.65 (4.61)	17.03 (9.20)	9.38 (9.09)	2.23 (1.13)	22.27 (16.38)	20.04 (17.43)	0.1	**0.008**	**0.03**	0.3
Ec.MAR (μm/day)	0.094 (0.163)	0.399 (0.338)	0.305 (0.442)	0 (0)	0.446 (0.327)	0.446 (0.327)	0.1	**0.05**	0.6	0.7

Male Data	WT Males (n=7)			Akita Males (n=5)			p Values of Pairwise Comparisons			
	nonloaded	loaded	Δ (loaded-nonloaded)	nonloaded	loaded	Δ (loaded-nonloaded)	WT Males (loaded vs. nonloaded)	Akita Males (loaded vs. nonloaded)	nonloaded ulnae (Akita vs. WT)	Δ (loaded-nonloaded) (Akita vs. WT)
Ec.BFR/BS ($\mu m^3/\mu m^2/day$)	0.010 (0.018)	0.110 (0.114)	0.100 (0.125)	0 (0)	0.155 (0.160)	0.155 (0.160)	**0.05**	**0.05**	0.6	0.7

Note: Data are presented as mean (standard deviation). Pairwise comparisons were performed using either Student's t tests (shaded with light blue) or Mann-Whitney U tests for normally or non-normally distributed data, respectively.